Reliable Transmission for Underwater Optical Wireless Communication Networks with Energy Harvesting

Cuong T. Nguyen*, Mat T. Nguyen†, Vuong V. Mai†, and Chuyen T. Nguyen*
* School of Electronics and Telecommunications, Hanoi University of Science and Technology, Vietnam
E-mail: cuong.nt160527@sis.hust.edu.vn, chuyen.nguyenthanh@hust.edu.vn
† Photonics Systems Research Lab., School of Electrical Engineering, KAIST, Korea
E-mail: mat.nt4656@kaist.ac.kr, m.v.vuong@ieee.org

Abstract—We study a reliable protocol of transmitting packets for underwater optical wireless communication networks. In the protocol, a probing packet is transmitted to predict the channel condition before transmitting a data packet. Energy harvesting is also activated during the protocol operation. A Markov chain model is proposed to theoretically analyze the protocol performance. Computer simulations are performed to validate the correctness of our analysis, as well as to show the efficiency of the protocol.

Index Terms—Underwater optical wireless communication (UWOC), error control, energy harvesting, probing mechanism, Markov chain.

I. INTRODUCTION

The internet of underwater things (IoUT), which is well known as a subclass of the internet of things (IoT), is expected to enable various important underwater applications such as mine and oil reconnaissance, disaster prevention, environmental monitoring, underwater surveillance, and intrusion detection [1], [2]. To support the concept of IoUT, underwater wireless sensor networks (UWSNs) have emerged as one of the most promising network systems [3]. UWSNs usually include multiple components such as vehicles and sensors. They might be deployed in a specific underwater area to perform collaborative monitoring and data collection tasks [4]. Despite huge potentials, several challenges such as long propagation delay, narrow bandwidth, low data rate caused by traditional acoustic communication still remain unsolved in the context of UWSNs.

To cope with those above issues, several approaches have been studied, among which underwater optical wireless communication (UOWC) has been recently considered as a possible candidate. Indeed, it has been proved in [5] that for a short-range distance, UOWC can provide much higher data rates with significantly lower power consumption and simpler computational complexities in comparison with acoustic communication systems. Nevertheless, the deployment of UOWC sensor networks also faces great challenges. In particular, underwater channel phenomena such as absorption, scattering, turbulence, water types, and interference might significantly degrade the reliability of signal transmission, which thus

reduces the attainable communication ranges and network performance efficiency [6]. Moreover, the limitation of energy consumption in sensor nodes is another key challenge, especially in underwater environments where battery replacing and recharging are very difficult.

A few of research activities have been investigated in UOWC for the issue of transmission reliability. In particular, a review of different modulation and coding schemes could be found in [5], while the authors in [7] discussed the effect of error correction coding schemes on system performance. Also, in [8], the performance of the UOWC system utilizing single photon avalanche diode detector was analyzed with turbulence effects, and automatic repeat request (ARQ) that enables packet retransmissions was applied to improve the reliability over extended distances. On the other hand, for the energy issue, energy harvesting (EH) technology was suggested as one of the most potential solutions [9]. All studies have been proven efficient both in terms of theoretical analysis and experiment deployment. Nevertheless, in those works, none of them could simultaneously solve both reliability and energy issues, which motivates us to propose this work.

The main contributions of this paper are as follows:

- We study a smarter way of transmitting packets, namely ARQ-P, for UOWC networks. Different from conventional ARQ, a probing packet (in basic energy level) is transmitted to predict the channel condition before a data packet (in higher energy level) is transmitted. Therefore, ARQ-P could (1) reduce the number of unsuccessful data-packet transmissions caused by unstable underwater optical channels, and (2) use energy more effectively. For further solving the energy issue, energy harvesting is also activated during the operation of ARQ-P.
- We propose a Markov chain model to theoretically analyze the throughput of ARQ-P. The correctness of our analysis is validated by Monte-Carlo simulations. The advantages of ARQ-P over conventional ARQ is shown through numerical results. The effects of energy harvesting and optimum parameter selection on ARQ-P are also provided.

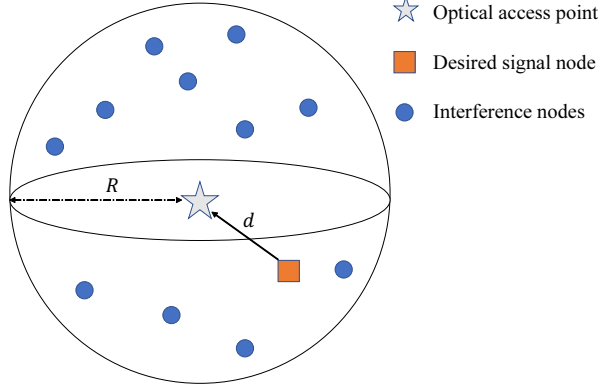## II. System Model

A. System description

Fig. 1: A 3-D model of underwater optical wireless sensor network.

Our system model, as depicted in Fig. 1, includes one omni-directional optical access point (OAP) [10], and $n+1$ sensor nodes that are uniformly distributed in a 3-dimensional area around the OAP specified by a radius of R. In the considered situation, the OAP tries to gather information from the desired node that is d meters far from the OAP under the interference from the other n nodes. The transmission between the OAP and each node is assumedly a point-to-point underwater optical wireless channel.

The system is studied in a time-division-multiple-access mode where a slot is defined as a necessary time that the desired node completes the transmission of one packet. Energy harvesting is employed, in which the node is equipped with a battery that has a maximum energy level of $E_{\max}$ units. In one time slot, the node can harvest one energy unit, save at the battery, and use the energy for the transmission. Also, for a data packet transmission during a time slot, it takes the same energy units denoted by E_{dtx} ($1 < E_{\mathrm{dtx}} < E_{\max}$) for simplicity. Here, energy harvesting and transmission are assumedly independent.

The considered node has two modes i.e., active and sleep, which is based on the battery's energy level. In particular, a node is at sleep mode when its energy level is below a threshold of E_{th} units, and in this case, the node drops out any current data packets and denies all requests. At the active mode where the energy level is higher than E_{th} units, the desired node performs its packet transmission. Here, the packet arrival assumedly follows a Poisson process with an average arrival rate of $\lambda_{\mathrm{packet}}$ (packets/time slot). If the packet is received correctly, an active acknowledgement (ACK) is sent back to the node, while a negative acknowledgement (NAK) is used, otherwise.

B. UOWC transmission model

According to [11], the signal-to-interference-plus-noise-ratio (SINR) in the considered model can be obtained as

$$\mathrm{SINR} = \frac{S \cdot [1 - \exp(-c(\lambda) - 4)n]}{I + N}, \tag{1}$$

where S, I and N are the signal, interference and noise components, respectively; $c(\lambda) = a(\lambda) + b(\lambda)$ is the extinction coefficient where $a(\lambda)$ and $b(\lambda)$ are the absorption and scattering coefficients, respectively. The noise component includes shot and thermal noises where the shot noise is written as

$$\sigma^2_{\mathrm{shot}} = 2q\gamma B \left(P_{r,s} + \sum_{i=1}^{n} P_{r,i} \right) + 2qI_{bg}I_2 B, \tag{2}$$

where γ is the Optical-to-Electrical (O/E) conversion efficiency; q is the electronic charge; B is noise bandwidth; $P_{r,s}$ is the received optical power from the from the desired signal power; $P_{r,i}$ is the received optical power from the i-th interference node; I_{bg} is the background current; I_2 is noise bandwidth factor. The thermal noise $\sigma^2_{\mathrm{thermal}}$ is defined as follows

$$\sigma^2_{\mathrm{thermal}} = \frac{8\pi k T_k}{G}\eta A_r I_2 B^2 + \frac{16\pi^2 k T_k \Gamma}{g_m}\eta^2 A_r^2 I_3 B^3, \tag{3}$$

where k is the Boltzmann's constant; T_k is the absolute temperature; G is the open-loop voltage gain; η is the fixed capacitance of photo detector per unit area; Γ is the FET channel noise factor; g_m is the FET transconductance. The interference component from n other nodes is also found as

$$I = nP_t\delta_t\delta_r \frac{A_r}{2\pi}\frac{3}{c(\lambda)R^3}\left(1 - \exp(-c(\lambda) \cdot R)\right), \tag{4}$$

where P_t is the optical transmitted power; δ_t and δ_r are the transmitter and receiver optical efficiency; A_r is the receiver aperture area. The signal component is given by

$$S = \gamma^2 \left(P_{r,s}\right)^2 = \gamma^2 \left(P_t\delta_t\delta_r \exp(-c(\lambda) d)\frac{A_r}{2\pi d^2}\right)^2. \tag{5}$$

On the other hand, under effects of the turbulence, the UOWC channel gain might follow exponentiated Weibull distribution according to [12]. In this case, and under all aperture averaging conditions [13], the system bit-error rate (BER) can be found as follows [14]

$$P_b = \frac{\alpha\beta\sqrt{k\pi}}{2\sigma(2\pi)^{\frac{\ell+k}{2}}}\left(\frac{\ell}{\sigma}\right)^{\frac{\beta}{2}-1}\sum_{j=0}^{\infty}\frac{(-1)^j\Gamma(\alpha)}{j!\Gamma(\alpha-j)} $$
$$\times G^{\,k,2\ell}_{2\ell,k+\ell}\left[\left(\frac{\omega_j}{k}\right)^k\left(\frac{\ell}{\sigma}\right)^\ell \middle| \begin{matrix}\Delta\left(\ell,1-\frac{\beta}{2}\right),\Delta\left(\ell,\frac{1}{2}-\frac{\beta}{2}\right)\\ \Delta(k,0),\Delta\left(\ell,-\frac{\beta}{2}\right)\end{matrix}\right], \tag{6}$$

where $\alpha > 0, \beta > 0$ are shape parameters; η is the scale parameter; $\omega_j = j + 1$; $\sigma = \frac{(\eta\mathrm{SINR})^2}{8}$; ℓ and k are integers that satisfy $\frac{\ell}{k} = \frac{\beta}{2}$; $\Delta(k,a)$ is a series of $\frac{a}{k}, \frac{a+1}{k}, \ldots, \frac{a+k-1}{k}$; $G^{\,m,n}_{p,q}[.]$ is known as the Meijer's G-function.

III. AUTOMATIC REPEAT REQUEST WITH PROBING (ARQ-P) PROTOCOL

A. Protocol description

In this section, an error control mechanism is proposed to cope with the unreliable UOWC transmission, which is based on probing and ARQ (stop-and-wait)[1] protocols. In particular, during each time slot, the desired node (in active mode, supposedly) first checks if there is a data packet to send. If there is not, the node waits for the next time slot. Otherwise, it will start its transmission by sending a probing packet to detect the channel condition. In this case, the node, depending on the corresponding feedback i.e., ACK or NAK, decides to send the data packet and wait for an acknowledgment, or to keep the transmission at the next time slot, respectively. It is noted here that, the channel is assumedly unchanged during each time slot where the transmission of both probing packet and data packet can be performed. This also implies that if the ACK of the probing packet is received, the data packet will be transmitted successfully.
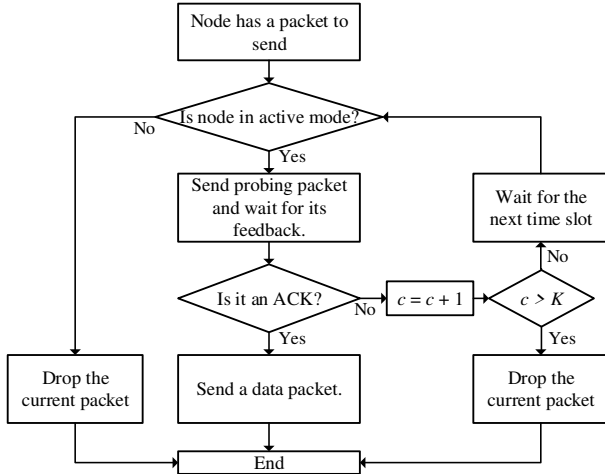

Fig. 2: Packet transmission of desired node with the proposed ARQ-P protocol (c is the retransmission counter initially set by 0).

On the other hand, if NAK is received, the node repeats the above transmission at the next time slots until it receives an ACK or the number of retransmissions reaches a threshold denoted by K. In this latter case, the current transmission (and thus, the data packet also) is dropped out. Moreover, forward error correction (FEC) mechanism is also employed in our work to improve the error control performance. In the mechanism, the maximum number of erroneous bits that can be detected and recovered is assumedly t bits. The proposed error control mechanism for packet transmission is summarized in Fig. 2. It is noted that energy harvesting is always activated at the desired node when ARQ-P is operating.

---

[1]Other types of ARQ protocol will be investigated in future works

B. Analysis of throughput performance

In this section, the performance of the proposed ARQ-P is theoretically analyzed in terms of system throughput defined as the average number of successfully transmitted bits in each time slot, as follows

$$\text{Throughput} = P_{\text{succ}} L, \tag{7}$$

where L is the data packet length in bits, and P_{succ} is the average probability that a packet is transmitted successfully during a time slot.

To find the P_{succ}, the performance of a packet transmission with the ARQ-P mechanism is modeled via a finite-state Markov chain as shown in Fig. 3. For a given time slot, each state i of the model is represented by two variables, namely $\{r, e\}$, in which r and e, respectively, denote by the number of retransmissions and the sensor node's energy level. Here, it is assumed that the total number of states is m. Different types of lines describe different performance where the solid lines, dashed lines, and dash-dotted lines respectively define processes of EH, the energy consumption of the unsuccessful transmission, and the energy consumption of the successful transmission. E_0 denotes by the initial energy level, and it is noted here that the minimum energy for a successful transmission is assumedly $E_{\text{th}} - E_0 + 1$ without loss of generality. $E_{\text{ptx}} = 1 + E_{\text{F}}$ is the amount of energy taken for a probing packet transmission where "1", as mentioned above, refers to the energy harvested during a time slot. The state transition when the node is active is expressed in detail in Fig. 3b where $E_{PP} = E_{\max} - K E_{\text{F}}$ and $E_S = E_{\text{dtx}} + E_{\text{ptx}} - 1$. Here, it is noted that due to the normalization of the EH scheme, E_{th}, E_{F}, E_{ptx}, E_{PP}, $E_{\max}$, E_S, E_{dtx}, and E_{ptx} are integers.

Using this model, P_{succ} can be written as follows

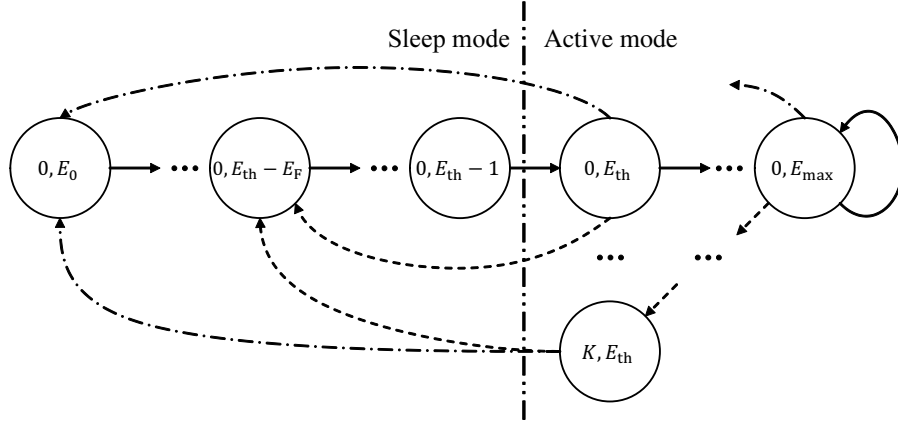$$P_{\text{succ}} = \sum_{i=0}^{m} \pi_i P_g(i)(1 - P_f), \tag{8}$$

where π_i is a stationary probability that the node is currently in state i; $P_g(i)$ is a probability that the node (in state i) has a packet to transmit, which is expressed as follows

$$P_g(i) = \begin{cases} \begin{cases} 1 - \exp(-\lambda_{\text{packet}}) & , r = 0 \\ 1 & , r \neq 0 \end{cases} & , E_{\text{th}} \leq e \leq E_{\max} \\ 0 & , E_0 \leq e < E_{\text{th}} \end{cases} \tag{9}$$
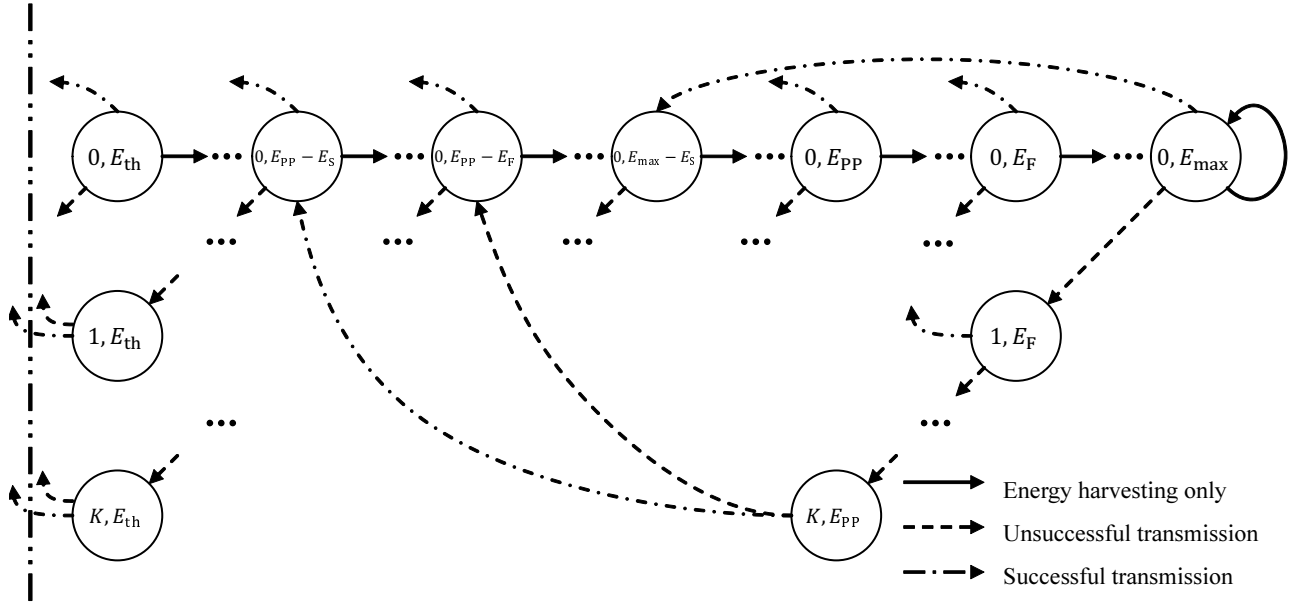
P_f is the frame error rate and can be found as

$$P_f = 1 - \sum_{p=0}^{t} \binom{L}{p} P_b^p (1 - P_b)^{L-p}, \tag{10}$$

where P_b is obtained from (6).

(a) The general state transition in ARQ-P.

(b) The detailed state transition in active mode in ARQ-P.

Fig. 3: Markov chain model of state transition for ARQ-P.

We are now going to find the probability vector $\boldsymbol{\pi} = [\pi_1, ..., \pi_m]$. In particular, according to Markov theory [15], we have

$$\begin{cases} \boldsymbol{\pi} \cdot \mathbf{Q} = \boldsymbol{\pi} \\ \sum_{i=1}^{m} \pi_i = 1, \end{cases} \quad (11)$$

where $\mathbf{Q}$ is a $m \times m$ transition probability matrix. In other words, $\mathbf{Q}_{i,j}$ denotes by a probability that the node, which is currently in state i, will be in state j at the next time slot. It can be found as follows

- If the node has no packet, it only harvests the energy (one energy unit) during a time slot, and thus

$$\mathbf{Q}_{\{0,e\}\{0,e+1\}} = \mathbf{Q}_{\{0,E_{\max}\}\{0,E_{\max}\}} = 1 - P_g(i). \quad (12)$$

Here, it is noted that if the energy level of the node was already maximum, it will be unchanged without transmission.

- If the node has a packet to send, it transmits a probing packet only if $E_{\text{th}} \leq e \leq E_{\max}$. If the transmission is successful, the data packet will be also received correctly. In this case, r is reset by 0, while the energy level is

TABLE I: Parameters used in simulation.

Parameters	Value
B	10 (MHz)
R	500 (m)
P_t	10 (W)
δ_r	0.9
δ_t	0.9
γ	0.54
A_r	0.01
q	1.6×10^{-19} (C)
T_k	298 ($^\circ K$)
k	1.38×10^{-23} (J/K)
I_2	0.562
G	10
Γ	1.5
g_m	30×10^{-3}
η	112×10^{-8}
I_3	0.0868
I_{bg}	5100 (μA)
L	128 bits
t	6 bits
E_0	1 energy unit
$E_{\max}$	40 energy units
E_S	6 energy units
E_F	1 energy units
λ_{packet}	0.2

Fig. 4: System throughput with ARQ and ARQ-P.

reduced by E_S energy units, as follows

$$\mathbf{Q}_{\{r,e\}\{0,e-E_S\}} = P_g(i)\left(1 - P_f\right). \quad (13)$$

- In case the probing packet transmission is unsuccessful, the energy is consumed by E_F units, and the node tries to retransmit the packet at the next time slot. It is noted here that the node only retransmits when $E_{\text{th}} + E_F \leq e \leq E_{\max}$, and if $E_{\text{th}} \leq e < E_{\text{th}} + E_F$, the node drops the packet and puts itself into the sleep mode. We have

$$\mathbf{Q}_{\{r,e\}\{r+1,e-E_F\}} = \mathbf{Q}_{\{r,e\}\{0,e-E_F\}} = P_g(i)P_f. \quad (14)$$

- When the node reaches the maximum number of retransmission while the transmission of the probing packet is still unsuccessful, it also drops the packet i.e.,

$$\mathbf{Q}_{\{K,e\}\{0,e-E_F\}} = P_f, \quad (15)$$

where $E_{\text{th}} \leq e \leq E_{\text{PP}}$. In the other cases, $\mathbf{Q}_{i,j} = 0$. After obtaining $\mathbf{Q}$, $\boldsymbol{\pi}$ and, thus, the throughput can be determined according to (11), (8), and (7).

IV. NUMERICAL RESULTS AND DISCUSSIONS

In this section, the ARQ-P performance is numerically evaluated by Monte-Carlo method with 100 iterations of 10^6 time slots. The parameters of the exponentiated Weibull fading channel are selected as in [14] i.e., $\alpha = 5.93, \beta = 0.46, \eta = 0.11$. The distance d is set by 6m. Other parameters are summarized in Table I.

Fig. 4 depicts the throughput for the number of interference nodes in clear ocean whose extinction coefficient ($c(\lambda)$) is 0.151 [16]. The energy harvesting rate during a time slot denoted by λ_{harvest} is set as 1 unit. It is seen that the analytical results completely match with the simulation one, which confirms the correctness of our above analysis. It is also observed that the 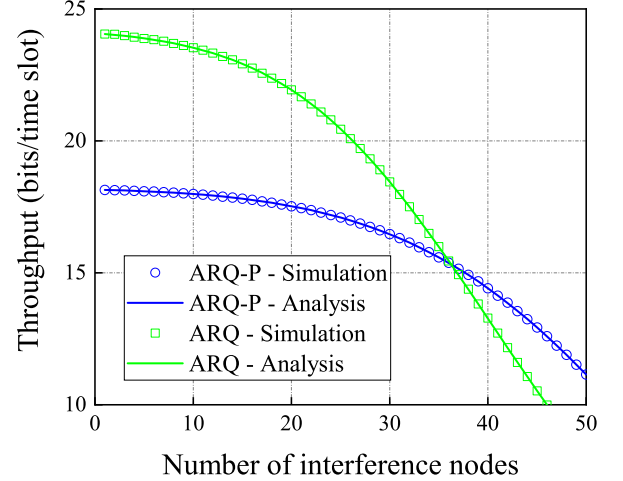throughput performance with ARQ is higher than that with ARQ-P when the number of interference nodes n is small ($n \leq 36$). Nevertheless, for a higher value of n, the proposed mechanism outperforms the conventional one. This is because, in unfavorable channel conditions of high interference, ARQ-P can reduce the unsuccessful transmission of data packets by using probing ones.
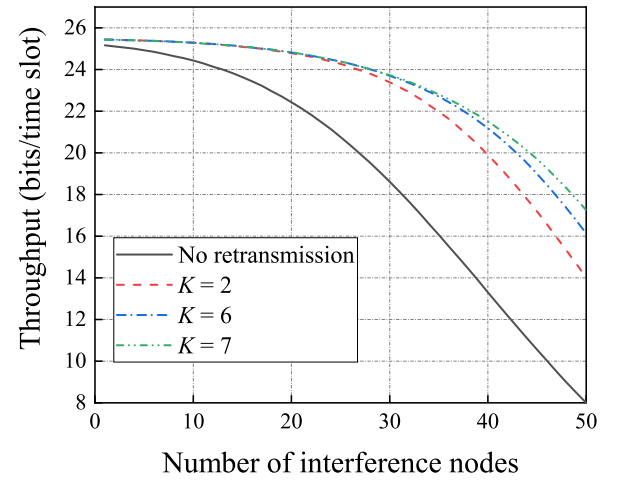
Fig. 5: System throughput with ARQ-P for different selections of K.

In Fig. 5, the system throughput with ARQ-P is plotted for different numbers of retransmissions K in the clear ocean. The energy harvesting rate of 2 units is set. The figure shows us that the system performance can be improved by using ARQ-P regardless of the number of interference nodes. Moreover, the results also recommend an optimal selection of K to obtain

the maximum throughput, while keeping K at a minimum value for satisfying other constraints of delay and energy consumption. For example, when $n \leq 30$, K can be set by 2.
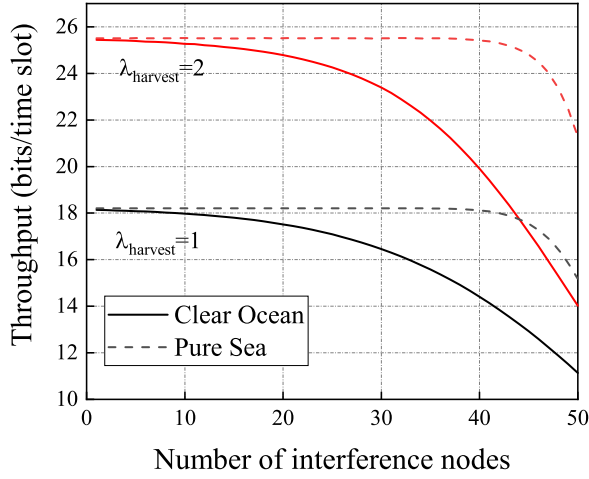

Fig. 6: System throughput with ARQ-P for different water types and different energy harvesting rates.

Finally, Fig. 6 describes the effect of different energy harvesting rates and different water types (in the pure sea water, $c(\lambda) = 0.056$) on the throughput performance with ARQ-P when $K = 2$. It is understandable that for a given water type, the more energy the node harvests, the more chance of retransmissions the node can perform. As a result, the throughput with the higher λ_{harvest} is higher than that with a lower one. Moreover, in pure sea water type, the effect of absorption and scattering on the signal transmission is smaller than that with clear ocean one. Therefore, the system throughput with pure sea shows higher values, regardless of λ_{harvest}.

V. Conclusions

In this paper, we studied a reliable transmission protocol for underwater optical wireless communication networks with energy harvesting scheme. Markov chain model was adopted to theoretically analyze the transmission performance in terms of system throughput. Computer simulations were also performed under different system parameter settings using the Monte-Carlo method, and the obtained results showed a good match between the analysis and simulation. They, besides, proved the effectiveness of the proposed mechanism in improving the throughput in unfavorable channel conditions. Moreover, the optimal selection of the number of retransmissions was also provided, which would be very useful for system designers in practical systems.

VI. Acknowledgement

References

[1] X. Zhang, J.-H. Cui, S. Das, M. Gerla, and M. Chitre, "Underwater wireless communications and networks: theory and application: Part 1 [guest editorial]," *IEEE Communications Magazine*, vol. 53, no. 11, pp. 40–41, 2015.

[2] I. F. Akyildiz, D. Pompili, and T. Melodia, "Underwater acoustic sensor networks: research challenges," *Ad hoc networks*, vol. 3, no. 3, pp. 257–279, 2005.

[3] C.-C. Kao, Y.-S. Lin, G.-D. Wu, and C.-J. Huang, "A comprehensive study on the internet of underwater things: applications, challenges, and channel models," *Sensors*, vol. 17, no. 7, p. 1477, 2017.

[4] K. M. Awan, P. A. Shah, K. Iqbal, S. Gillani, W. Ahmad, and Y. Nam, "Underwater wireless sensor networks: A review of recent issues and challenges," *Wireless Communications and Mobile Computing*, vol. 2019, no. 1, pp. 1–20, 2019.

[5] H. Kaushal and G. Kaddoum, "Underwater optical wireless communication," *IEEE access*, vol. 4, no. 4, pp. 1518–1547, 2016.

[6] N. Saeed, A. Celik, T. Y. Al-Naffouri, and M.-S. Alouini, "Underwater optical wireless communications, networking, and localization: A survey," *Ad Hoc Networks*, vol. 94, p. 101935, 2019.

[7] J. A. Simpson, W. C. Cox, J. R. Krier, B. Cochenour, B. L. Hughes, and J. F. Muth, "5 mbps optical wireless communication with error correction coding for underwater sensor nodes," in *Proceedings of OCEANS*, 2010, pp. 1–4.

[8] T. Shafique, O. Amin, M. Abdallah, I. S. Ansari, M.-S. Alouini, and K. Qaraqe, "Performance analysis of single-photon avalanche diode underwater vlc system using arq," *IEEE Photonics Journal*, vol. 9, no. 5, pp. 1–11, 2017.

[9] S. Sudevalayam and P. Kulkarni, "Energy harvesting sensor nodes: Survey and implications," *IEEE Communications Surveys & Tutorials*, vol. 13, no. 3, pp. 443–461, 2010.

[10] G. Baiden, Y. Bissiri, and A. Masoti, "Paving the way for a future underwater omni-directional wireless optical communication systems," *Ocean Engineering*, vol. 36, no. 9-10, pp. 633–640, 2009.

[11] M. T. Nguyen, V. V. Mai, and C. T. Nguyen, "Sinr performance analysis of 3-d underwater optical wireless communication networks," in *2019 26th International Conference on Telecommunications (ICT)*, 2019, pp. 41–45.

[12] M. V. Jamali, A. Mirani, A. Parsay, B. Abolhassani, P. Nabavi, A. Chizari, P. Khorramshahi, S. Abdollahramezani, and J. A. Salehi, "Statistical studies of fading in underwater wireless optical channels in the presence of air bubble, temperature, and salinity random variations," *IEEE Transactions on Communications*, vol. 66, no. 10, pp. 4706–4723, 2018.

[13] R. Barrios and F. Dios, "Exponentiated weibull model for the irradiance probability density function of a laser beam propagating through atmospheric turbulence," *Optics & Laser Technology*, vol. 45, no. 1, pp. 13–20, 2013.

[14] R. Barrios Porras *et al.*, "Exponentiated weibull fading channel model in free-space optical communications under atmospheric turbulence," Ph.D. dissertation, Universitat Politècnica de Catalunya.

[15] M. A. Berger, "Markov chains—stationary distributions and steady state," in *An Introduction to Probability and Stochastic Processes*. Springer, 1993, pp. 101–120.

[16] B. Cochenour, L. Mullen, and A. Laux, "Spatial and temporal dispersion in high bandwidth underwater laser communication links," in *Proceedings of IEEE Military Communications Conference (MILCOM)*. IEEE, 2008, pp. 1–7.